IOPscience iopscience.iop.org

Home Search Collections Journals About Contact us My IOPscience

Hydrostatic-pressure effects on the donor binding energy in GaAs–(Ga, Al)As quantum dots

This article has been downloaded from IOPscience. Please scroll down to see the full text article.

2007 J. Phys.: Condens. Matter 19 026225

(http://iopscience.iop.org/0953-8984/19/2/026225)

View the table of contents for this issue, or go to the journal homepage for more

Download details:
IP Address: 129.252.86.83
The article was downloaded on 28/05/2010 at 15:21

Please note that terms and conditions apply.

INSTITUTE OF PHYSICS PUBLISHING JOURNAL OF PHYSICS: CONDENSED MATTER

J. Phys.: Condens. Matter **19** (2007) 026225 (7pp) doi:10.1088/0953-8984/19/2/026225

Hydrostatic-pressure effects on the donor binding energy in GaAs–(Ga, Al)As quantum dots

S T Perez-Merchancano[1], **H Paredes-Gutierrez**[2] **and J Silva-Valencia**[3]

[1] Departamento de Física, Universidad del Cauca, Popayán, Colombia
[2] Escuela de Física, Universidad Industrial de Santander, A A 678, Bucaramanga, Colombia
[3] Departamento de Física, Universidad Nacional de Colombia, A A 5997, Bogotá, Colombia

E-mail: sperez@unicauca.edu.co, hparedes@uis.edu.co and jsilvav@unal.edu.co

Received 6 June 2006, in final form 30 November 2006
Published 15 December 2006
Online at stacks.iop.org/JPhysCM/19/026225

Abstract
The binding energy of shallow hydrogenic impurities in a spherical quantum dot under isotropic hydrostatic pressure is calculated using a variational approach within the effective mass approximation. The binding energy is computed as a function of hydrostatic pressure, dot size and impurity position. The results show that the impurity binding energy increases with the pressure for any position of the impurity. Also, we have found that the binding energy depends on the location of the impurity and the pressure effects are less pronounced for impurities on the edge.

1. Introduction

Low dimensional systems have been studied intensively in the last decades [1]. Examples of these systems are single and multiple quantum wells, superlattices, quantum wires and quantum dots. Some of these elements are part of several current electronic devices [2]. The optical and transport properties of semiconductors are sensitive to impurities, external fields and stress; therefore, it is important to consider these aspects in heterostructures. The pioneering work by Bastard [3] on the binding energy of a donor hydrogenic impurity in a quantum well has been extended to quantum well wires and quantum dots [4–6, 8].

Perez-Merchancano *et al* [5] and Zhu *et al* [7] made the first study of the confinement effects on the impurity states (donor and acceptor) in quantum dots. They calculated the binding energies for the ground and excited states as a function of dot size and impurity position. The more realistic zero dimensional quantum heterostructure (cubic dot) was studied by Ribeiro and Latgé [9]. They found that the values of donor binding energies for cubic and spherical quantum dots are very close, provided that the dots have similar volumes.

Diverse experimental techniques allow the fabrication of quantum dots. Using the masked implantation enhanced intermixing technique, and the dry etching technique with subsequent overgrowth, Schweizer *et al* [10] have realized rectangular transversal section

0953-8984/07/026225+07$30.00 © 2007 IOP Publishing Ltd Printed in the UK

GaAs–(Ga, Al)As quantum well wires and quantum dots. Also spherical colloidal monocrystals of CdTe has been made [11].

In recent years, the hydrostatic pressure effect on band structure of bulk material and low dimensional systems has been considered both theoretically and experimentally. In particular, when the hydrostatic pressure is applied to either bulk GaAs or $In_xGa_{1-x}As$ alloy, a crossing of two or more of the conduction band electronic levels occurs. The Γ-point conduction band minimum increases relative to the valence band maximum with increasing pressure. Simultaneously, the X-point energy level decreases. At a crossover pressure P_C, the Γ and X levels cross and the material goes from being k space direct to indirect. This is referred to as the Γ–X crossover [12, 13]. Elabsy [14] has calculated the effect of hydrostatic pressure on the binding energy of donor impurities in quantum well heterostructures, and found that the binding energy increases with increasing external hydrostatic pressure for a given quantum well thickness and temperature.

Photoluminescence studies of self-organized InAlAs/AlGaAs quantum dots under pressure were carried out by Phillips *et al* [15]. The effect of hydrostatic pressure on the optical transitions in self-assembled InAs/GaAs quantum dots was studied by Duque *et al* [16]. Oyoko *et al* [17] studied donor impurities in a parallelepiped-shaped GaAs–(Ga, Al)As quantum dot and they found that the donor binding energy increases with increasing uniaxial stress and decreasing sizes of the quantum dot. On the other hand, donor impurities in a spherical quantum dot with parabolic confinement potential under hydrostatic pressure were considered by Gerardin Jayam and Navaneethakrishnan [18] and they found that the hydrostatic pressure increases the donor ionization energy such that the variation is larger for a smaller dot.

In the present work, we investigate the effects of hydrostatic pressure on the binding energies of off-centre shallow donor impurities in a spherical quantum dot, using the variational method within the effective mass approximation.

2. Theory

In the effective mass approximation, the Hamiltonian of a hydrogenic shallow-donor impurity in a spherical quantum dot of GaAs–(Ga, Al)As, under the influence of hydrostatic pressure within, is given by

$$H = \frac{\mathbf{P}^2}{2m^*(P)} - \frac{e^2}{\varepsilon(P)|\mathbf{r}-\mathbf{r}_0|} + V(r, P) \tag{1}$$

where $m^*(P)$, $\varepsilon(P)$ and $V(r, P)$ are the effective mass of an electron, the static dielectric constant and the confining potential respectively. Note that the above quantities depend explicitly on the hydrostatic pressure. In the Hamiltonian (1), $\mathbf{r}_0$ denotes the impurity position inside a dot of radius $R = R(P)$, which also depends on the hydrostatic pressure. The confinement potential $V(r, P)$ in the Hamiltonian (1) is given by

$$V(r, P) = \begin{cases} 0 & r \leqslant R(P) \\ V_0(P) & r \geqslant R(P). \end{cases} \tag{2}$$

The boundary conditions on the wavefunctions are that $\psi(r)$ and its first normal derivative are continuous at the potential boundary. The eigenfunctions of the Hamiltonian (1) in the absence of the impurity are

$$\psi_{10}(\mathbf{r}) = \begin{cases} N_0 \dfrac{\sin(\zeta_{10} r)}{r}, & r \leqslant R(P) \\ N_0 \dfrac{\sin(\zeta_{10} r)}{r} e^{\chi_{10}(R-r)}, & r \geqslant R(P) \end{cases} \tag{3}$$

with

$$\zeta_{10} = \left[\frac{2m^*(P)E_{10}}{\hbar^2}\right]^{1/2}, \tag{4}$$

and

$$\chi_{10} = \left[\frac{2m^*(P)\,(V_0(P) - E_{10})}{\hbar^2}\right]^{1/2}, \tag{5}$$

where E_{10} is the energy of the ground state given by the transcendental equation

$$-\left(\frac{V_0(P)}{E_{10}} - 1\right)^{-1/2} = \tan(\zeta_{10}R(P)). \tag{6}$$

Equation (3) is the wavefunction of a particle confined in a finite spherical potential well. The inclusion of the impurity potential makes it necessary to use a variational approach to approximate the wavefunctions and eigenvalues implied by the Hamiltonian. Taking into account the spherical confining geometry and the hydrogenic impurity potential, we use the trial wavefunction

$$\psi(\mathbf{r}) = \begin{cases} N\dfrac{\sin(\zeta_{10}r)}{r}\mathrm{e}^{-\lambda|\mathbf{r}-\mathbf{r}_0|}, & r \leqslant R(P) \\ N\dfrac{\sin(\zeta_{10}r)}{r}\mathrm{e}^{\chi_{10}(R-r)}\mathrm{e}^{-\lambda|\mathbf{r}-\mathbf{r}_0|}, & r \geqslant R(P). \end{cases} \tag{7}$$

The binding energy $E_\mathrm{b}(R, r_0)$ of the hydrogenic impurity is defined as the ground-state energy of the system when the impurity is absent, minus the impurity ground-state energy $\xi(R, r_0)$, i.e.,

$$E_\mathrm{b}(R, r_0) = \frac{\hbar^2}{2m^*(P)}\zeta_{10}^2 - \xi(R, r_0, P). \tag{8}$$

The application of hydrostatic pressure modifies the lattice constants, dot size, barrier height, effective masses and dielectric constants. Next, we displayed the explicit expressions for these quantities as a function of the hydrostatic pressure, where pressure is in kbar. The variation of the well width with pressure is given by

$$R(P) = R_0(1 - 1.5082 \times 10^{-4}P), \tag{9}$$

where R_0 is the zero pressure width of the quantum dot, taking into account $(\mathrm{d}a/\mathrm{d}P) = -2.6694 \times 10^{-4}a_0$, where a_0 is the lattice constant of GaAs [19]. The variation of dielectric constant with the pressure is given as

$$\varepsilon(P) = 13.13 - 0.0088P; \tag{10}$$

this expression was determined from refractive index measures at $T = 300$ K [20].

The effective mass in the well and barrier regions changes as

$$m^*(P) = m^*(0)\exp(0.0078P); \tag{11}$$

here $m^*(0) = 0.067m_0$ is the effective mass without pressure and m_0 is the bare electron mass [21].

We assume that the bandgap discontinuity in a GaAs–$Ga_{1-x}Al_xAs$ quantum dot heterostructure is distributed about 40% on the valence band and 60% on the conduction band, with the total bandgap difference $\Delta E_\mathrm{g}(x, P)$ (in eV) between GaAs and $Ga_{1-x}Al_xAs$ given as a function of the Al concentration $x < 0.45$ and the hydrostatic pressure P as

$$\Delta E_\mathrm{g}(x, P) = \Delta E_\mathrm{g}(x) + PD(x) \tag{12}$$

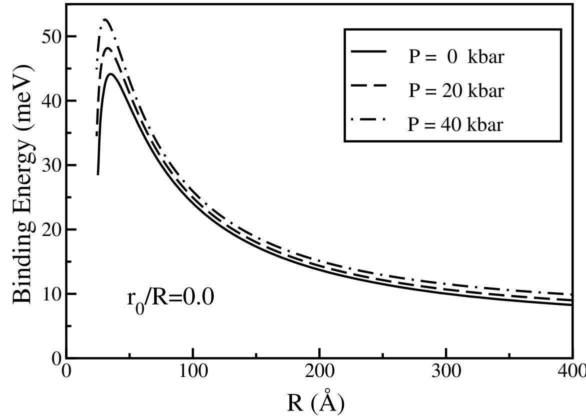

Figure 1. Binding energy of an on-centre donor impurity in a GaAs–(Ga, Al)As quantum dot as a function of the dot radius for different pressures.

where

$$\Delta E_g(x) = 1.155x + 0.37x^2 \quad (13)$$

is the variation of the energy gap difference without pressure and $D(x)$ (in eV kbar^{-1}) is the pressure coefficient of the bandgap given by [21]

$$D(x) = -(1.3 \times 10^{-3})x. \quad (14)$$

Then the height of the potential barrier for shallow donor impurities as a function of Al concentration x and the hydrostatic pressure is given by

$$V_0(P) = 0.6\Delta E_g(x, P); \quad (15)$$

here we consider the Al concentration equal to $x = 0.30$.

With these variations the donor binding energy is obtained, for different pressures and dot sizes, using the variational method within the effective mass approximation.

3. Results and discussion

Figure 1 shows the binding energy for an on-centre donor impurity as a function of the quantum dot radius, for three different hydrostatic pressure values, which are $P = 0$, 20 and 40 kbar, respectively. The behaviour of the binding energies without pressure ($P = 0$) is similar to the previous results found in [3–5]. For all pressures we observe that the binding energy increases from its bulk value in GaAs as the dot radius is reduced, reaches a maximum value, and then drops to the bulk value characteristic of the barrier material as the dot radius goes to zero. This behaviour of the binding energy as a function of the well size for finite barrier heterostructures is known. Note that the binding energy increases with the hydrostatic pressure for any dot radius, reflecting the additional confinement due to the pressure; this is in agreement with the results obtained previously [17, 18]. Also, we observe that the pressure effect is more appreciable for narrow dots, and the maximum position goes to small radius when the pressure increases.

On the other hand, in figure 2 we present the binding energy as a function of the quantum dot radius for different impurity positions. Here we consider a hydrostatic pressure $P = 20$ kbar, and the impurity is located at $r_0/R = 0$ (on-centre), $r_0/R = 0.5$ (on-middle) and $r_0/R = 1.0$ (on-edge). The behaviour of the binding energy with the radii for the off-centre

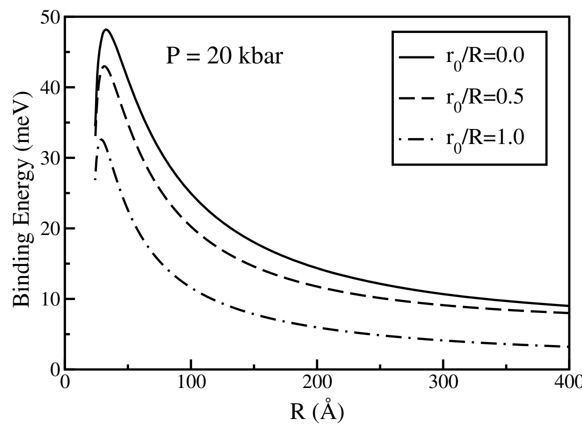

Figure 2. Binding energy of an on-centre and off-centre donor impurity in a GaAs–(Ga, Al)As quantum dot as a function of the dot radius under a pressure $P = 20$ kbar.

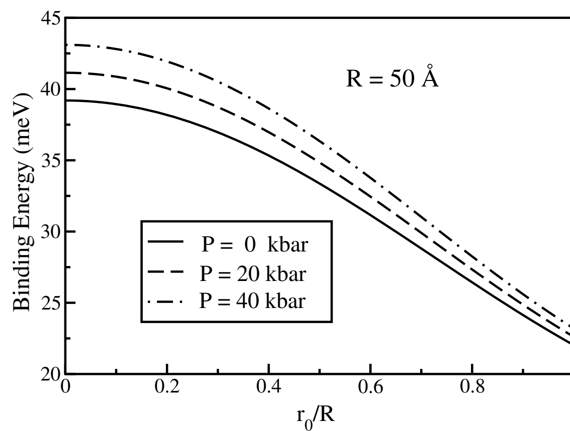

Figure 3. Binding energy of a donor impurity in a GaAs–(Ga, Al)As quantum dot of radii $R = 50$ Å as a function of the impurity position. Three different pressure values are considered.

impurity is similar to the on-centre case. Given any dot radius we can see that the binding energies decrease when the impurity is displaced from the centre. Also, the maximum position goes to small radius when the impurity tends to the edge.

The dependence of binding energy on the impurity position inside a quantum dot of radii $R = 50$ Å is shown in figure 3 for three different pressure values $P = 0$, 20 and 40 kbar. In each case, the binding energy for on-edge impurities is lower than for the on-centre impurity. The binding energy decreases continuously as the position of the impurity moves away from the centre, reaching a minimum on the edge; this is in agreement with the results obtained previously [22, 8]. In addition, we notice from this plot that for any impurity position inside the dot the binding energy increases with the pressure. The hydrostatic pressure effects are seen to be more appreciable for impurities away from the edge; there, the repulsion of the wavefunction by the potential barrier is relevant and it diminishes the confinement effect due to the hydrostatic pressure.

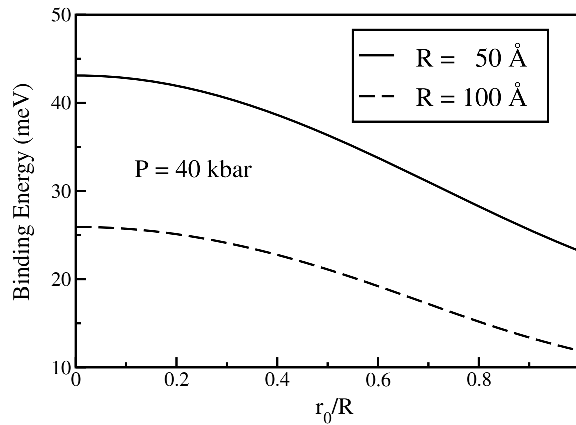

Figure 4. Donor binding energy as a function of the impurity position for GaAs–(Ga, Al)As quantum dots of radii $R = 50$ and 100 Å.

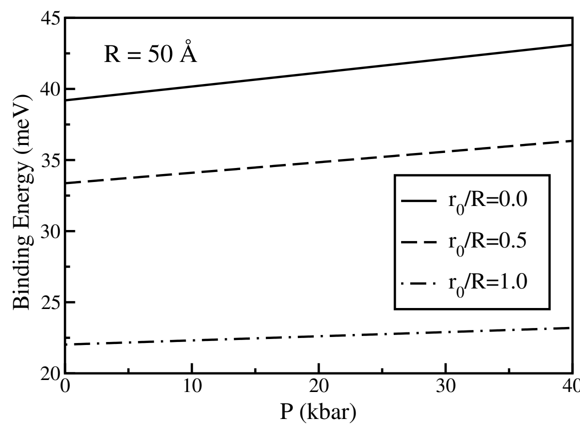

Figure 5. Donor binding energy as a function of the pressure for a GaAs–(Ga, Al)As quantum dot of radius $R = 50$ Å. Three different impurity positions are considered.

Figure 4 shows the binding energy as a function of the donor position inside the quantum dot for finite potential wells with different radii. The hydrostatic pressure is constant and equal to $P = 40$ kbar. The donor binding energy decreases as the donor position increases, reaching a minimum when the donor position is equal to the radius of the quantum dot. It can further be noted from this figure that the variation in the binding energy with the impurity position is more pronounced for smaller dots. This observation is in agreement with the results reported in [22] without pressure and [17] with pressure. In this work we do not consider the non-parabolic effects, which are important for small dots.

Furthermore, the variation of the binding energy with pressure is shown in figure 5. Here we consider a quantum dot of radius $R = 50$ Å and three different impurity positions, $r_0/R = 0$ (on-centre), $r_0/R = 0.5$ (on-middle) and $r_0/R = 1.0$ (on-edge). The binding energy shows a nearly linear increase with the pressure. Note that the slope of the curve depends on the impurity position and the smaller value is found on the edge. This curve tell us that a system that operates under hydrostatic pressure may be used to tune the output of optoelectronic devices without

modifying the physical size of the quantum dot. We have not considered pressures beyond 40 kbar, because of a direct to indirect bandgap transition for GaAs at about 40 kbar [23].

During the revision of the paper, we became aware of the new expressions for the lattice constants, dot sizes, barrier heights, effective masses and dielectric constants as a function of temperature and hydrostatic pressure [24]. Nevertheless, our main results are not significantly modified if these expressions are used.

4. Summary

To summarize, the binding energy of donor impurities inside a spherical GaAs–(Ga, Al)As quantum dot increases with the hydrostatic pressure for any position of the impurity. The radius of the quantum dot with maximum binding energy depends on the pressure and the impurity position. The hydrostatic pressure effects are less pronounced for impurities on the edge. The slope of the curve of binding energy versus pressure depends on the impurity position.

Acknowledgments

STP-M would like to thank the VRI-Universidad del Cauca. This work was partially financed by Colombian Agencies Colciencias (grant No 1101-333-18707) and Universidad Nacional de Colombia (DINAIN-20601003550 and DIB-8003060).

References

[1] Bimberg D, Grudmann M and Ledentsov N N 1999 *Quantum Dot Heterostructures* (New York: Wiley)
[2] Davies John H 1998 *The Physics of Low Dimensional Semiconductors: an Introduction* (Cambridge: Cambridge University Press)
[3] Bastard G 1981 *Phys. Rev.* B **24** 4714
[4] Brown J and Spector N 1986 *J. Appl. Phys.* **59** 1179
[5] Porras-Montenegro N and Perez-Merchancano S T 1992 *Phys. Rev.* B **46** 9780
[6] Porras-Montenegro N, Perez-Merchancano S T and Latgé A 1993 *J. Appl. Phys.* **74** 7624
[7] Zhu J L, Xiong J J and Gu B L 1990 *Phys. Rev.* B **41** 6001
[8] Movilla J L and Planelles J 2005 *Phys. Rev.* B **71** 075319
[9] Ribeiro F J and Latgé 1994 *Phys. Rev.* B **50** 4913
[10] Schweizer H, Lehr G, Prins F, Mayer G, Lach E, Kruger R, Frohlich E, Pilkuhm M H and Smith G W 1992 *Superlatt. Microstruct.* **12** 419
[11] De Giorgi M, Tarì D, Manna L, Krahne R and Cingolani R 2005 *Microelectron. J.* **36** 552
[12] Elabsy A M 1994 *J. Phys.: Condens. Matter* **6** 10025
Elabsy A M 1993 *Superlatt. Microstruct.* **14** 65
[13] Burnett J H, Cheong H M, Paul W, Koteles E S and Elman B 1993 *Phys. Rev.* B **47** 1991
[14] Elabsy A M 1993 *Phys. Scr.* **48** 376
[15] Phillips J D, Bhattacharya P K and Venkateswaran U D 1999 *Phys. Status Solidi* b **211** 85
[16] Duque C A, Porras-Montenegro N, Barticevic Z, Pacheco M and Oliveira L E 2006 *J. Phys.: Condens. Matter* **18** 1877
[17] Oyoko H O, Duque C A and Porras-Montenegro N 2001 *J. Appl. Phys.* **90** 819
[18] Gerardin Jayam Sr and Navaneethakrishnan K 2003 *Solid State Commun.* **126** 681
[19] Benedictal A, Sukumar B and Navaneethakrishnan K 1993 *Phys. Status Solidi* b **178** 167
[20] Goni A R, Syassen K and Cardona M 1990 *Phys. Rev.* B **41** 10104
[21] Adachi S 1985 *J. Appl. Phys.* **58** R1
[22] Silva-Valencia J and Porras-Montenegro N 1997 *J. Appl. Phys.* **81** 901
[23] Wolford D J and Bradly J A 1985 *Solid State Commun.* **53** 1069
[24] Herbert Li E 2000 *Physica* E **5** 215